



## **FISH & CHIPS: Single Chip Silicon MEMS CTDL Salinity, Temperature, Pressure and Light sensor for use in fisheries research**

**Hyldgård, Anders; Hansen, Ole; Thomsen, Erik Vilain**

*Published in:*  
Proceedings of MEMS 2005

*Link to article, DOI:*  
[10.1109/MEMSYS.2005.1453927](https://doi.org/10.1109/MEMSYS.2005.1453927)

*Publication date:*  
2005

*Document Version*  
Publisher's PDF, also known as Version of record

[Link back to DTU Orbit](#)

*Citation (APA):*  
Hyldgård, A., Hansen, O., & Thomsen, E. V. (2005). FISH & CHIPS: Single Chip Silicon MEMS CTDL Salinity, Temperature, Pressure and Light sensor for use in fisheries research. In *Proceedings of MEMS 2005* (pp. 303-306). IEEE. <https://doi.org/10.1109/MEMSYS.2005.1453927>

---

### **General rights**

Copyright and moral rights for the publications made accessible in the public portal are retained by the authors and/or other copyright owners and it is a condition of accessing publications that users recognise and abide by the legal requirements associated with these rights.

- Users may download and print one copy of any publication from the public portal for the purpose of private study or research.
- You may not further distribute the material or use it for any profit-making activity or commercial gain
- You may freely distribute the URL identifying the publication in the public portal

If you believe that this document breaches copyright please contact us providing details, and we will remove access to the work immediately and investigate your claim.

# FISH & CHIPS: SINGLE CHIP SILICON MEMS CTDL SALINITY, TEMPERATURE, PRESSURE AND LIGHT SENSOR FOR USE IN FISHERIES RESEARCH

A. Hyldgård, O. Hansen, and E.V. Thomsen

Technical University of Denmark, Dept. of Micro and Nanotechnology (MIC), Lyngby, Denmark

## ABSTRACT

A single-chip silicon MEMS CTDL multi sensor for use in aqueous environments is presented. The new sensor chip consists of a conductivity sensor based on platinum electrodes (C), an ion-implanted thermistor temperature sensor (T), a piezo resistive pressure sensor (D for depth/pressure) and an ion-implanted p-n junction light sensor (L). The design and fabrication process is described. A temperature sensitivity of  $0.8 \times 10^{-3} \text{K}^{-1}$  has been measured and detailed analysis of conductivity measurement data shows a cell constant of  $81 \text{cm}^{-1}$ .

## 1. INTRODUCTION

In recent time a significant focus has been set on fish behaviour and fish population estimations due to the expected endangerment of certain species of fish mainly as a result of excessive fishing activity. Reliable monitoring of individual fish behaviour and migration in their natural environment is crucial in order to make accurate population estimations and plans for preservation of the different species.

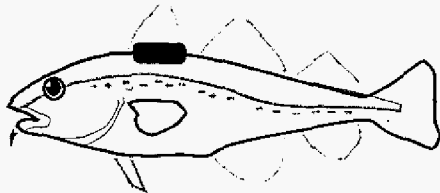


Figure 1: A cod with a Data Storage Tag sutured onto its back. The considerable size of current tags sets the lower limit for the size of the fish that can be tagged.

Data Storage Tags (DSTs) are small autonomous measuring systems that offer to deliver precise information about the fish surroundings. When a fish is caught the DST is sutured to its back (see Figure 1) and the fish is released. For a period of time the DST measures parameters in the fish surroundings and stores the data in an internal memory. When fishermen re-catch the fish, an award is offered for the return of the DST, and researchers can then retrieve the measured data.

The usefulness of current DSTs is strongly limited by the size, price and limited measuring capabilities. The DSTs comprise of a sensor part, interface electronics, a non-volatile memory and a energy source as depicted in Figure 2. The aim of our project is to increase measuring capabilities and to shrink the system size while keeping in mind that the design is only a complete success if tags can be produced at a price comparable or preferably lower than that of the DSTs available today.

By making an integrated multi-sensor and applying custom made electronics and packaging concept the total system size can be shrunk to a size mainly limited by the size of the needed energy source. The emphasis of this paper is on the design and fabrication of multi-sensor chips capable of measuring depth, temperature, salinity and light intensity. From well-established polynomial fits to empirical data of the conductivity, temperature and pressure, the salinity can be calculated [1]. The light intensity day variation can be used to deduct the longitude and latitude. This information can be used to reconstruct fish migration and fish patterns of behaviour.

The new multi-sensor chip implements, unlike conventional sensor systems, all sensors needed to make salinity measurements at high-pressure (e.g. at deep-sea), where the conductivity data has to be pressure compensated to ensure accurate salinity results.

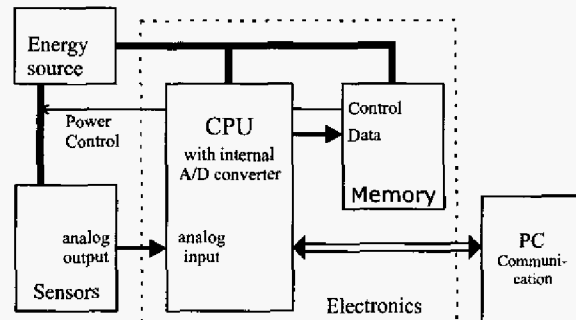


Figure 2: Schematics of the Data Storage Tag subparts. The sensors can be integrated into one chip and the electronics on another. The volume of a complete system will ultimately be limited by the onboard energy source.

## 2. DESIGN

The chip has been designed so that it can be exposed directly to the seawater in order to gain a high level of accuracy and low response times. A reliable O-ring packaging concept as depicted in Figure 3 is used, and a protective film is applied to the chip surface. The chip packaging concept with a compressed O-ring and a protective film has proven very reliable in other harsh environments [2] and should offer excellent protection.

The chip size is  $4 \times 6 \text{mm}^2$  and the sensors are placed as central on the chip as possible in order to minimize the influence from stress that unavoidably will be introduced from the packaging. The chip can easily be shrunk to  $4 \times 4 \text{mm}^2$  in final production by rearranging the contact areas to the corners of the square chip.

The pressure sensor consists of a  $50 \mu\text{m}$  thick,  $800 \mu\text{m}$  square membrane with four piezo resistors

( $N_A=2.2 \times 10^{18} \text{cm}^{-3}$ ) arranged in a Wheatstone bridge configuration. The resistors are placed so that the resistor value will pair wise increase and decrease to give a linear bridge output signal from 0-20 bar with a resolution of about 0.1 bar.

The temperature sensor is also made as a Wheatstone resistor bridge with the resistor doping concentration tuned to give a negative and positive temperature response.  $N_A=5 \times 10^{16} \text{cm}^{-3}$  gives a temperature coefficient of resistance (TCR) of  $3.6 \times 10^{-3} \text{K}^{-1}$  and  $N_A=2.2 \times 10^{18} \text{cm}^{-3}$  gives a TCR of  $-0.5 \times 10^{-3} \text{K}^{-1}$ . The output to input signal ratio will thus have a sensitivity of approx.  $2 \times 10^{-3} \text{K}^{-1}$ . This results in a possible resolution of at least 0.01K for a 3V input voltage.

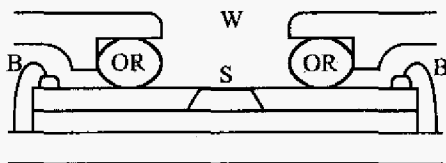


Figure 3: Cross-section of the O-ring packaging concept. The sensor-chip area (S) is exposed directly to the water (W) through the O-ring (OR). Wire-bonds (B) make electrical connections to the interface electronics.

A set of electrodes exposed directly to the seawater functions as an electrical conduction sensor cell. To measure the conductivity of an electrolyte it is necessary to use AC voltages, because of dominant capacitances at the electrode-electrolyte interface. The electrodes are dimensioned on the basis of a FEM model and capacitive considerations in order to ensure that a change in electrical conductivity in the water can be observed at medium frequencies as described in the results section. The design allows for both two- and four-probe measurements.

The light sensor is a p-n junction diode with a  $0.37 \text{mm}^2$  junction area. Fortunately, silicon is a strong absorber at the blue wavelengths where seawater transmits light. This makes light measurements possible at a depth lower than 100m in clear seawater.

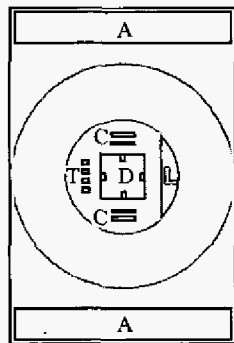


Figure 4: Chip design layout. The sensors; Temperature (T), Pressure (D), Electrical conductivity (C) and Light intensity (L), are centred with respect to the interface O-ring. The contact areas (A) are placed on the dry ends of the chip.

All sensors are electrically connected to contact pads at the edge of the chip. The very compact placement of the sensors yields a need for low sheet resistance interconnects that can be placed under a protective film. A silicide serves this purpose as well as light shielding of the sensor areas, to eliminate light sensitivity for the implanted pressure and temperature sensors. Furthermore, silicide combined with implanted conductors allows for crossover of electrical interconnects. The chip layout is depicted in Figure 4.

### 3. FABRICATION

Figure 5 shows a cross-sectional fabrication sequence for the multi-sensor chip. Different resistors optimized for piezo resistivity, thermal sensitivity and high conductivity, respectively, are ion-implanted through a silicon dioxide layer into the single crystal silicon (100) substrate. The resistive sensors have a resistance of approx.  $30 \text{k}\Omega$  to yield low power consumption while keeping a high signal to noise ratio.

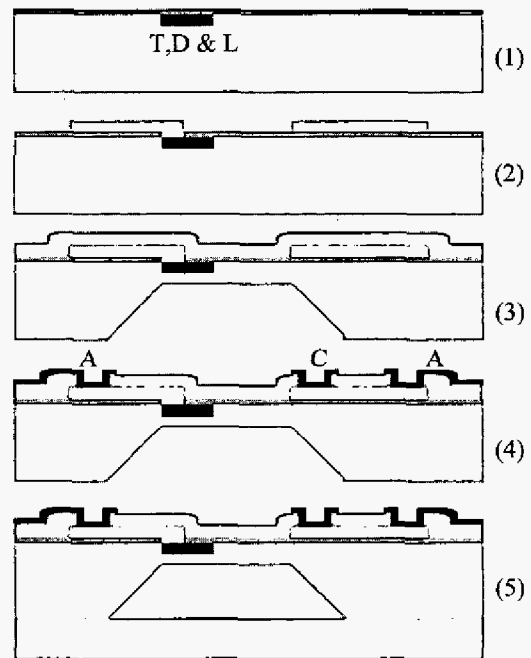


Figure 5: Chip fabrication sequence. (1) Sensors (T,D & L) are ion implanted. (2)  $\text{TiSi}_2$  wiring is formed. (3)  $\text{Si}_3\text{N}_4$  coating is applied and a membrane etched out. (4) Two metallizations form electrodes (C) and contact areas (A). (5) A Pyrex wafer is anodic bonded to the backside.

The implanted resistors are contacted via a  $\text{TiSi}_2$  wiring system made by RTP annealing of titanium and polysilicon. The low sheet resistance of the  $\text{TiSi}_2$  wiring ensures low parasitic series resistances between sensors and contacts even in long conductor paths ( $R_s=1\Omega$ ). Both sides of the wafer are coated with a LPCVD silicon nitride. The nitride is used as masking material in the subsequent KOH bulk silicon etch that forms the pressure sensor membrane. The backside nitride is then removed

whereas the front-side nitride is kept as the protective coating of the sensors. Contact holes are made through the nitride by reactive ion etching.

The chips are metallized by platinum and gold to form electrodes and contact pads respectively as the demands for corrosion inertness and wire bonding compatibility are not met by a single metal. The backside of the chip is anodic bonded to a Pyrex wafer to form a low-pressure reference cavity and add mechanical stability to the chip.

The complete process is only slightly more complex than processes used in commercial pressure sensor fabrication, and is well suited for batch processing. A finished chip is shown in Figure 6.

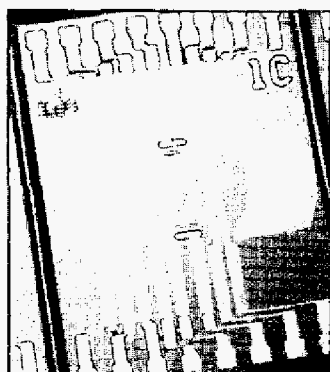


Figure 6: Picture of the  $4 \times 6 \text{ mm}^2$  multi-sensor chip. The dark paths are titanium silicide conductors and the light areas are gold used for bonding-pads and electrodes. The front-side is protected by a  $\text{Si}_3\text{N}_4$  film.

#### 4. RESULTS

Piezo resistive pressure sensors and p-n junction photo diodes are well described in literature and the performance is well known. The light sensor shows a linear response to light intensity but a measure of noise and quantum efficiency is needed to evaluate the performance of the sensor. The emphasis here will be on the electrical conductivity measurements and the temperature sensor. These are also the most important parameters when determining the salinity.

##### Temperature

The temperature sensor has been tested in an air heated oven using a K-type thermo couple (TC) for the reference temperature probe. The measured temperature range is higher than the expected working range, but it shows that leakage currents are not a problem. As the data in Figure 7 indicates there must be a slight time delay between the TC and the chip sensor as the heating and cooling curve differ. The results were reproducible so the difference is not drift related.

The slight non-linearity is partly due to the change in temperature coefficient of resistance of the sensor with temperature and partly due to a slightly unbalanced Wheatstone bridge. For sea investigations the above

deviations should give no problems, since the expected temperature variations are limited and the heat transport more efficient. The sensor sensitivity of  $0.8 \times 10^{-3} \text{ K}^{-1}$  is approximately 40% of the expected value. This could be caused by a deviation in actual doping level from the design value or that the temperature model is not accurate enough in this range.

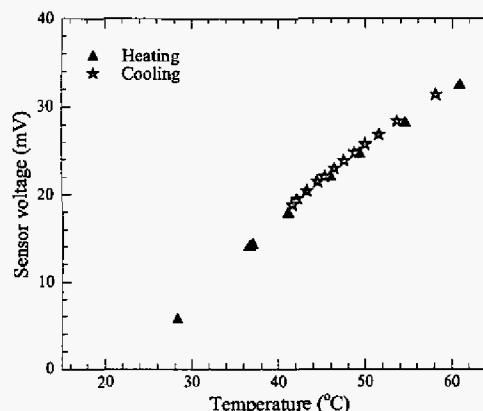


Figure 7: The temperature sensor voltage as a function of reference temperature measured with a thermocouple. For small changes in temperature the dependence is almost linear.

##### Electrical conductivity

In the ideal case the cell impedance  $Z$  is related to the water conductivity  $\kappa$  through the equation

$$Z = \frac{K}{\kappa}$$

where the cell constant  $K$  depends on the cell geometry. However, due to parasitic capacitances in the substrate and electrolytic double layer capacitances forming in the water at the electrode interface [3], the measured cell impedance has to be compensated. A simplified equivalent circuit of  $Z$  is shown in Figure 8.  $Z_E$  expresses the electrolysis process and is much higher than the water impedance  $Z_W$ .  $Z_W$  and the double layer capacitance  $C_{DL}$  depend on the electrode area. The cell is designed to make  $C_{DL}$  and  $Z_W$  high while keeping the parasitic capacitance  $C_P$  low.

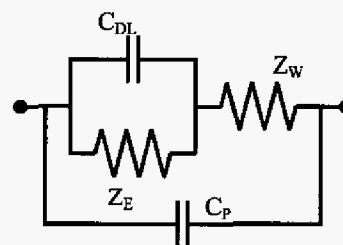


Figure 8: Conductance cell equivalent circuit. The electrolysis impedance  $Z_E$  is much higher than the water impedance  $Z_W$ . The double layer capacitance  $C_{DL}$  is higher than the parasitic capacitance  $C_P$ .

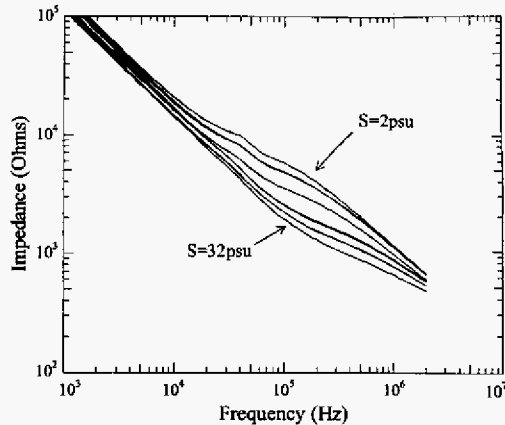


Figure 9: Cell impedance at 6 different salinities (2, 4, 8, 16, 24 and 32psu) as a function of frequency. For each salinity value approx 10 measurements are super-imposed.

Figure 9 shows the cell impedance vs. frequency for 6 different salinities. The impedance depends strongly on salinity at frequencies between 50kHz and 500kHz. By plotting the cell impedance vs.  $1/f^2$  and extrapolating to infinite frequency the water impedance ( $Z_w$ ) can be deduced from the intersection with the impedance axis (Figure 10). The deduced water conductance ( $1/Z_w$ ) shows a linear dependence on the reference conductivity measured with a Radiometer CDC749 probe, as depicted in Figure 11. The offset stems from the parasitic conductance that is also experienced with no water in the cell. The deduced cell constant  $K$  for extrapolated data is  $81\text{cm}^{-1}$  which compares well with FEM results. The cell conductance is also linear dependent on water conductivity when measured at a single frequency. The best sensitivity is found at  $f=493\text{kHz}$  giving an effective  $K$  of  $68\text{cm}^{-1}$ . The extrapolation method should deliver accurate results even when the capacitance changes due to algae growth etc.

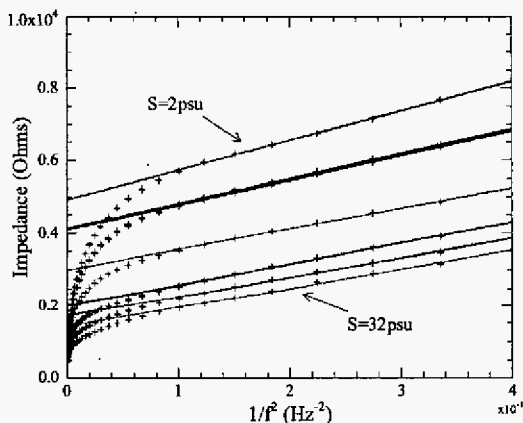


Figure 10: Measured cell impedance as a function of  $1/f^2$  at 6 different salinities (2, 4, 8, 16, 24 and 32psu). For each salinity value approx 10 measurements are super-imposed. Extrapolation to infinite frequency eliminates the double layer contribution.

A PSpice model (Figure 8) is fitted to the experimental data and the extracted capacitances are in good agreement with the expected theoretical values. The extracted double layer capacitance  $C_{DL}$  is  $1\mu\text{F}$  which compares well with an estimate of  $3\mu\text{F}$  based on typical values [3]. An extracted parasitic capacitance  $C_P$  of  $170\text{pF}$  compares well with  $70\text{pF}$  estimated from device geometry.

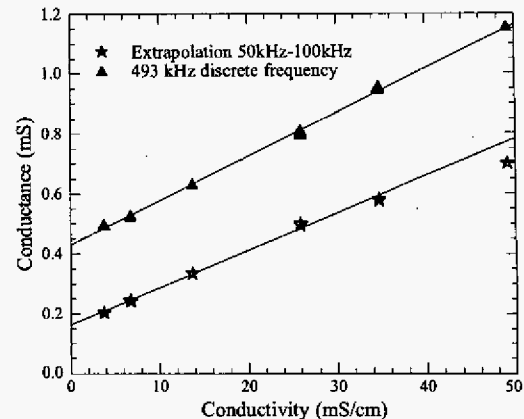


Figure 11: Measured cell conductance as a function of conductivity measured with a Radiometer CDC749 probe. Good linearity is found at a single frequency measurement ( $\blacktriangle$ ) as well as by extrapolating to infinite frequency ( $\star$ ).

## 5. CONCLUSIONS

The temperature sensor shows a linear response with a high signal to noise ratio. As expected, the p-n junction short circuit current is also linear with the light intensity. The conductivity sensor shows a linear response for both single frequencies and for extrapolation compensation. In conclusion, the multi-sensor chip offers precise determination of salinity, temperature, pressure and light intensity, and is a major step towards a new generation of miniturized DSTs.

## Acknowledgements

This work is supported by *The Danish Institute for Fisheries Research*.

## 6. REFERENCES

- [1] E. L. Lewis, "The Practical Salinity Scale 1978 and its antecedents", *IEEE Journal of Oceanic Engineering*, OE4:3-8, 1980
- [2] C. Pedersen, S. T. Jespersen, K. W. Jacobsen, J. P. Krog, C. Christensen, and E. V. Thomsen, "Highly Reliable O-ring Packaging Concept for MEMS Pressure Sensors", *Sensors and Actuators A* 115 (2004) 617-627
- [3] M. I. Montenegro et al, "Microelectrodes: Theory and applications", Kluwer Academic Publishers
- [4] E. Hunter et al, "Geolocation of free-ranging fish on the European continental shelf as determined from environmental variables", *Marine Biology*, 142-3 (2003), pp 601-609